Probing the validity of the Derjaguin approximation for heterogeneous colloidal particles

Samuel Rentsch, Ramon Pericet-Camara, Georg Papastavrou and Michal Borkovec*

Received 13th February 2006, Accepted 13th March 2006
First published as an Advance Article on the web 24th April 2006
DOI: 10.1039/b602145j

The Derjaguin approximation states that the interaction force between two curved surfaces is proportional to their effective radius, whereby the inverse effective radius is the arithmetic mean of the inverse curvature radii of the surfaces involved. The present study investigates the validity of this approximation with an atomic force microscope (AFM) by measuring interaction forces between colloidal particles of different sizes, but of identical composition. Forces were measured between silica particles of 2.0, 4.8 and 6.8 μm in diameter in KCl electrolyte solution with and without adsorbed poly(amido amine) (PAMAM) dendrimers. The Derjaguin approximation could be confirmed at all distances investigated, including those comparable with the characteristic length scales of the surface roughness or the surface charge heterogeneities. For the conditions investigated, the Derjaguin approximation turns out to be surprisingly robust.

Introduction

Interaction forces between colloidal particles dictate many important suspension properties, such as phase behavior, osmotic pressure, rheology or colloidal stability.[1–5] The interaction forces are commonly described by the classical theory of Derjaguin, Landau, Verwey, and Overbeek (DLVO), which superposes electrostatic forces due to the diffuse layer overlap and van der Waals interactions.[1,2] In many situations, interaction forces are influenced by other contributions, such as forces originating from heterogeneous surface charge distributions, surface roughness,[2,6–8] or, in the presence of polymers, steric or depletion interactions.[1,9,10]

Interaction forces are commonly evaluated from the interaction free energy of two infinite plates. Derjaguin has shown more than half a century ago that the force $F(D)$ between two bodies at a given surface separation distance D can be expressed in terms of the corresponding plate–plate interaction free energy per unit area $W(D)$ as[2,11]

$$F(D) = 2\pi R_{\mathrm{eff}}\, W(D) \qquad (1)$$

where the effective radius R_{eff} is given by

$$\frac{1}{R_{\mathrm{eff}}} = \frac{1}{R_1} + \frac{1}{R_2} \qquad (2)$$

where R_1 and R_2 are the curvature radii of both bodies at the point of closest approach. Eqn (1) is commonly referred to as the Derjaguin approximation (see Fig. 1a). It is applicable as long as the range of the interaction and the separation distance is small compared to the radii of curvature. These conditions are usually met in practice, and thus the Derjaguin approximation became one of the cornerstones in the interpretation of colloidal interactions.

The region of validity of the Derjaguin approximation has been investigated for different types of interactions in substantial detail theoretically.[1,6,7,9,12,13] The textbook example is the non-retarded van der Waals force between two spheres.[1] Since the exact expression for this force is known, the Derjaguin approximation can be verified to hold for $D \ll R_1, R_2$. It breaks down for distances that are comparable to, or larger than, the particle radii. In the case of interactions between charged surfaces across electrolyte solutions, its validity has been studied at the Poisson–Boltzmann level.[6,7,12] The Derjaguin approximation was found to be valid provided $D \ll R_1$, R_2 and $\kappa^{-1} \ll R_1, R_2$, where κ is the inverse Debye length, and

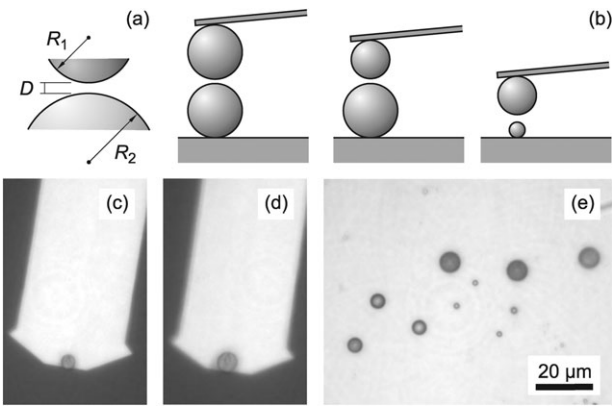

Fig. 1 Probing the Derjaguin approximation by the colloidal probe technique. (a) Definition of the geometrical parameters. (b) Variation of the effective radius R_{eff} by measuring the interaction forces between particles of different size. Optical micrograph of silica particles attached to the cantilever with diameters of (c) 4.8 μm and (d) 6.8 μm. (e) Substrate with attached spheres of 2.0, 4.8 and 6.8 μm in diameter.

Department of Inorganic, Analytical, and Applied Chemistry, University of Geneva, 1211 Geneva 4, Switzerland. E-mail: michal.borkovec@unige.ch

it was noted that it remains excellent over a relatively wide parameter range.[6,12] This approximation was further shown to be applicable for overall neutral, but heterogeneously charged spheres at separation distances smaller than the length scale of the surface heterogeneities.[7] This approximation was equally investigated for depletion interactions in hard-sphere mixtures.[9] One concludes that the approximation is valid for sufficiently small size ratios. The surface element integration was further proposed as an approximate scheme to calculate interaction forces for various geometries outside the validity regime of the Derjaguin approximation.[13]

In spite of these theoretical efforts, the validity of the Derjaguin approximation has been hardly investigated experimentally. Direct force measurements with the surface forces apparatus (SFA) or the colloidal probe technique are normally reported relative to the effective radius R_{eff} (*cf.* eqn (2)). With the SFA, the interaction forces are measured between two curved mica plates in the crossed-cylinder geometry.[2,14,15] The colloidal probe technique, which is based on an atomic force microscope (AFM), uses a colloidal particle of a few micrometers, attached to the end of the cantilever to probe the interaction force with a planar substrate (sphere-plane geometry)[10,15–21] or with a second colloidal particle mounted to the substrate (sphere–sphere geometry).[22–26] While any of these techniques could be used to assess the validity of the Derjaguin approximation, to the best of our knowledge there is only one study addressing this question.[27] These authors use sharp AFM tips for study interactions with planar surfaces, and report its breakdown.

We have decided to address this question with the colloidal probe technique in the sphere–sphere geometry. The technique has the advantage that the system is intrinsically symmetric and the particle radius can be varied by choosing the same type of colloidal particles of different sizes. In particular, we have investigated its validity for heterogeneous surfaces.

2. Experimental

2.1 Materials

Aqueous suspensions of spherical silica particles, which were synthesized according to the Stöber process, were purchased from Bangs Laboratories in three different size classes (see Table 1). The silica particles were heated for 24 h at 800 °C, whereby they remained a flowing powder. The heat treatment leads to more reproducible results than with unheated particles. Poly(amido amine) dendrimers of generations G3, G6, and G10 have been obtained from Dendritech (Midland, MI) and were used as received. All aqueous solutions were prepared from deionized water (Millipore). The solution pH and ionic strength values were adjusted by addition of HCl, KOH, and KCl, respectively.

Table 1 Properties of colloidal silica particles

Lot number	Mean diameter/μm[a]	RMS roughness/nm[b]
5252	2.0	<4.3
4908	4.8	2.1
4907	6.8	1.8

[a] Mean diameter according to the supplier. [b] Root mean square (RMS) roughness as determined by tapping mode AFM.

2.2 Sample preparation

The colloidal probes were prepared from tip-less AFM cantilevers (CSC12, μ-mach, Lithonia), which have been cleaned for 5 min in air-plasma at 18 W (PDC 32G, Harrick Scientific, NY). Colloidal silica particles with 4.8 and 6.8 μm in diameter were attached to the cantilevers with UV-curable glue (Optical Adhesive 63, Norland Products) using a micromanipulator (Märzhäuser). The same colloidal particles of 2, 4.8 and 6.8 μm in diameter were similarly glued to microscope glass slides (Menzel-Gläser, Germany) cleaned according to the RCA-method.[28] Thereby, the slides were immersed into a mixture of deionized water, ammonium hydroxide 30%, hydrogen peroxide 30% in a ratio of 5 : 1 : 1 by volume at 70–80 °C for 10 min and then amply rinsed with deionized water. Colloidal probes and substrates with attached particles were finally cleaned in an air plasma for 90 s. Optical micrographs of the colloidal probes and of the particles attached to the substrates are shown in Fig. 1.

For some experiments, the colloidal particles were modified by adsorption of cationic dendrimers. The colloidal probes and the substrates with attached spheres were immersed for at least 12 h in a solution of poly(amido amine) (PAMAM) dendrimers of 10 mg L^{-1} in 50 mM KCl electrolyte at pH 4. At these conditions the dendrimers are fully charged[29] and are known to adsorb strongly to oppositely charged surfaces.[30,31] The adsorption has reached saturation after 12 h. When such a dendrimer-coated surface is in contact with pure electrolyte solution, the adsorption is irreversible within the experimental time window. This fact has been verified under similar conditions by AFM imaging and time-resolved reflectometry. The silica surfaces are quite hydrophilic, as indicated by a contact angle around $\theta \simeq 10°$ of a RCA-cleaned quartz wafer. Adsorbed dendrimers make the surfaces slightly more hydrophilic ($\theta \simeq 7°$). For imaging, dendrimers were adsorbed by the same procedure onto silicon wafers in 5 and 50 mM KCl at pH 4.

2.3 AFM imaging

The surface topography of the heat-treated silica particles was investigated by tapping mode AFM in air (Multimode Nanoscope III, Veeco, CA). These measurements were performed with standard tapping cantilevers (OMCL-AC160TS, Olympus) with a tip radius below 12 nm. These cantilevers were selected by imaging a Nioprobe standard (Aurora Nanodevices, Edmonton, Canada). The particle topography was imaged in a frame of 1 × 1 μm around the center of the particle. The roughness was determined from images of least four different particles from the same batch, which were obtained by subtracting a sphere-cap fit or by flattening by third order polynomials. The results were expressed as the root mean square (RMS) deviation, and they were the same for both methods within experimental error. The particle roughness remains unaffected by the heating processes. The PAMAM dendrimers G10 were imaged on silica particles

and silicon wafers by tapping-mode AFM in the dry state with a damping ratio of 80%. Topographic and phase images were acquired simultaneously.

2.4 Direct force measurements

A closed-loop AFM (MFP-3D, Asylum Research, CA) mounted on an inverted optical microscope (Olympus IX 70) was used to measure the forces between the differently sized colloidal particles attached to the cantilever and the substrate (see Fig. 1b). The measurements were carried out in open petri dishes at pH 9.5 for the bare silica spheres and at pH 4.0 for the dendrimer coated samples. During a typical measurement time of 4 h, the pH value remained constant within 0.2. The particles on the probe and on the substrate were first coarsely aligned with optical microscopy. The fine alignment was achieved by scanning a square grid with a spacing of 100–200 nm in repeated approach and retraction cycles. The necessary vertical travel distance of the piezo-element to obtain a deflection value of 0.2 V was recorded. This value corresponds to a force of about 1 nN. The resulting distances were fitted to a sphere cap, which permits the horizontal alignment to a precision of better than 50 nm. The subsequent force measurements were carried out under feedback for the lateral position, and the corresponding drift is expected to lie below 10 nm during a typical 20 min measurement. There were no significant differences between the measurements between fully centered spheres, and when they were intentionally displaced 200 nm off center. This observation indicates that the mutual alignment of the two spheres is sufficiently accurate and is not critical.

After horizontal alignment, the forces in the vertical direction were determined by averaging at least 100 approach and retraction cycles with a frequency of 0.3 Hz, corresponding to an approach velocity of 0.8 μm s^{-1}. Force–distance curves were calculated from the cantilever deflection and the piezo displacement. The separation distance D is obtained from a linear fit of the constant compliance region, and has an accuracy of about 0.5 nm for the bare silica surfaces, and about 2 nm for the surfaces covered with dendrimers. The force F is determined from the deflection of the cantilever and its spring constant. The overall sensitivity in the force measurements is estimated to about 20 pN. The spring constants of the AFM cantilevers were determined by the added mass method, whereby the shift of the resonance frequency was investigated as a function of the added mass of attached tungsten particles, which were in the size range of 5–20 μm.[32] The resulting values in the range of 0.03–0.11 N m^{-1} were within 30% of the values determined by analyzing the thermal fluctuations in air[33] or the ones obtained with procedure proposed by Sader *et al.*,[34] which uses properties of the cantilever and the surrounding medium. The deviations between the values obtained by the different methods are probably due to the finite spot size of the laser beam on the cantilever, which leads to additional contributions from the higher order harmonics.[35] The particle radii were determined with optical microscopy with a precision of about 0.3 μm. Further details on the direct force measurements are given elsewhere.[18,19]

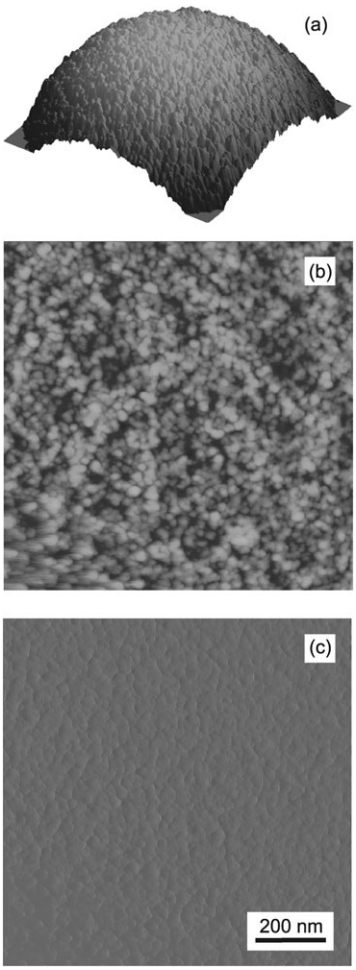

Fig. 2 AFM images of a bare silica particle of 4.8 μm in diameter. Topographic image in (a) stereographic projection and (b) when flattened with a third order polynomial. (c) Phase image with a phase lag scale from 0 to 50°, whereby the bright parts represent the areas with a high phase lag.

3. Results and discussion

The validity of the Derjaguin approximation was assessed experimentally by studying interaction forces between pairs of differently sized colloidal silica particles by the colloidal probe technique (see Fig. 1). We examined two different systems, namely bare silica particles in the diameter range of 2–7 μm, and the same particles with adsorbed poly (amido amine) (PAMAM) dendrimers. In both systems, the ionic strength was about 0.1 mM. The first system permits conclusions concerning the influence of the surface roughness, while the second illustrates effects of surface charge heterogeneities.

3.1 Interaction forces between bare silica particles

AFM images of typical silica particles with 4.8 μm in diameter are shown in Fig. 2. The substantial surface roughness becomes apparent already in the 3-D projection. The root mean square (RMS) of the residual surface roughness was 2.0 ± 0.2 nm (see Table 1). These numbers are well comparable to the RMS values of 1–2 nm reported for silica particles

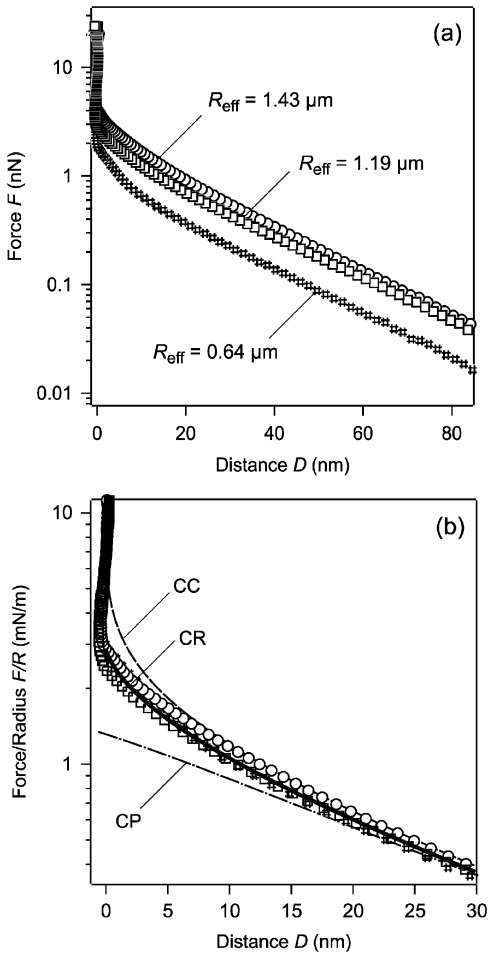

Fig. 3 Forces between pairs of silica particles as a function of the separation distance D across 0.1 mM aqueous KCl solution adjusted to pH 9.5. (a) Forces F for three different effective radii R_{eff}. (b) The same force profiles normalized to the effective radius F/R_{eff}. Lines are best fits with the PB model with constant charge (CC), constant potential (CP), and constant regulation (CR). The fitted parameters are summarized in Table 2.

previously.[25] For the smallest particles, somewhat larger values were observed, but this deviation could be an artifact due to the finite curvature of the sample. For the bare silica particles, the phase image reveals no additional features.

The interaction forces between pairs of silica particles were measured in the vertical direction by averaging the results of different approach and retraction cycles in an 0.1 mM KCl solution adjusted to pH 9.5. The ionic strength of the solution was 0.13 mM. The particles were centered relative to each other with a precision of at least 50 nm, which is sufficiently accurate as verified by additional off-center measurements. The approach and retraction cycles were fully reversible.

Typical results are shown in Fig. 3a. The measurements were carried out with a probe particle of 4.8 μm in diameter against particles attached to the substrate with diameters of 1.74 μm (R_{eff} = 0.64 μm), 4.8 μm (R_{eff} = 1.19 μm), and 7.0 μm (R_{eff} = 1.43 μm). At larger distances, the repulsion originates from the overlap of the diffuse layers, which compensates the negative surface charge of silica. We observe that the forces remain repulsive even at short distances and there are no indications of attractive van der Waals forces. These observations are fully in accord with previous studies.[36,37] The short-ranged repulsion is commonly interpreted to originate from the steric overlap of gel-like layers consisting of polysilicidic acid tails protruding from the surface.[37] The finite thickness of this layer displaces the plane of origin of the diffuse layer outwards, and the van der Waals force is weakened because of the substantial water content of this layer.[36]

Fig. 3b shows the measured interaction forces normalized to the effective radius. The normalized force profiles F/R_{eff} are compared to the solutions of the Poisson–Boltzmann equation for two infinite symmetric plates. Besides the classical boundary conditions of constant charge (CC) and constant potential (CP), we further consider the constant regulation approximation (CR).[38] For larger separations, the different boundary conditions yield the same force profile, and the diffuse layer potential and decay length can be estimated unambiguously. The fitted decay length of 23 nm coincides reasonably well with the expected Debye length of 27 nm, which was calculated from the Debye and Hückel theory with an ionic strength of 0.13 mM.[2] The observed deviation is probably caused by traces of dissolved carbonates originating from the air. The fitted diffuse layer potential is −83 mV (see also Table 2). The sign of the potential cannot be determined from force measurements, but silica is known to be negatively charged from potentiometric titrations, electrophoresis and streaming potential measurements.[25,39–41] As shown in Table 3, the presently observed value is well comparable with the ones reported by others at similar experimental conditions.[26,42,43]

At separations comparable to the Debye length and smaller, neither the constant charge nor the constant potential boundary conditions provide a good description of the force profiles. On the other hand, the constant regulation approximation provides an excellent fit of the data almost down to contact; that is to distances of 1–3 nm. The fitted surface potential and decay lengths are summarized in Table 2, while the resulting regulation parameter p = 0.52 suggests that the surfaces do regulate its charge upon approach significantly. For silica, surface charging models predict a similar range of the regulation parameter.[44]

The Derjaguin approximation stipulates that the force should be proportional to the effective radius (*cf.* eqns (1) and (2)). This approximation can be tested by varying the size

Table 2 Interpretation of direct force measurements by the Poisson–Boltzmann theory

System[a]	pH	Ionic strength mM	Debye length κ^{-1}/nm		Diffuse layer potential[c] mV
			Theor.[b]	Exp.[c]	
Bare silica	9.5	0.13	27	23	−83
PAMAM dendrimers G3	4.0	0.20	21	21	+68
PAMAM dendrimers G6	4.0	0.20	21	21	+98
PAMAM dendrimers G10	4.0	0.20	21	23	+70

[a] Measured in 0.1 mM KCl solution with adjusted pH. [b] Theoretical value based on the solution composition. [c] From force measurements with a relative error of about 10%.

Table 3 Literature comparison of diffuse layer potential for silica

Added salt	pH	Ionic strength/mM	Diffuse layer potential/mV	Ref.
KCl	9.5	0.13	−83	Present work
NaCl	9.5	0.20	−84	Toikka *et al.*[42]
KNO_3	9.0	0.11	−105	Larson *et al.*[43]
KNO_3	9.0	0.21	−73	Considine *et al.*[26]

of the probe particles or of the ones fixed to the substrate. Fig. 3b shows that the interaction force profiles normalized to the effective radius, F/R_{eff}, collapse rather well, which gives already a first confirmation of the Derjaguin approximation.

The validity of the Derjaguin approximation can be assessed in a better way by plotting the force F at a fixed distance as a function of the effective radius R_{eff} (*cf.* eqn (2)). These two quantities should be simply proportional to each other. Fig. 4 shows such plots whereby the solid lines are linear fits to the data with zero intercept. Indeed, the interaction forces are proportional to the effective radius for all distances considered, and the Derjaguin approximation is therefore fulfilled.

Fig. 4a and 4b compare the data for larger and smaller distances. Their comparison shows that the Derjaguin approximation holds even at small distances, which are comparable to the roughness of the silica spheres of 2–4 nm. Thus, even at the smallest distances the effect of the roughness is negligible. While the scatter of the data points increases on the scale of the graph, the relative error remains below 20%. Secondly, the force profiles measured during the individual approach and retraction cycles differ slightly, since the horizontal position cannot be maintained to sufficient precision on the scale of the surface roughness. Nevertheless, the scatter between individual force curves remains small, even at small distances.

3.2 Interaction forces between particles with adsorbed dendrimers

Heterogeneously charged surfaces were prepared by adsorption of positively charged PAMAM dendrimers of generations

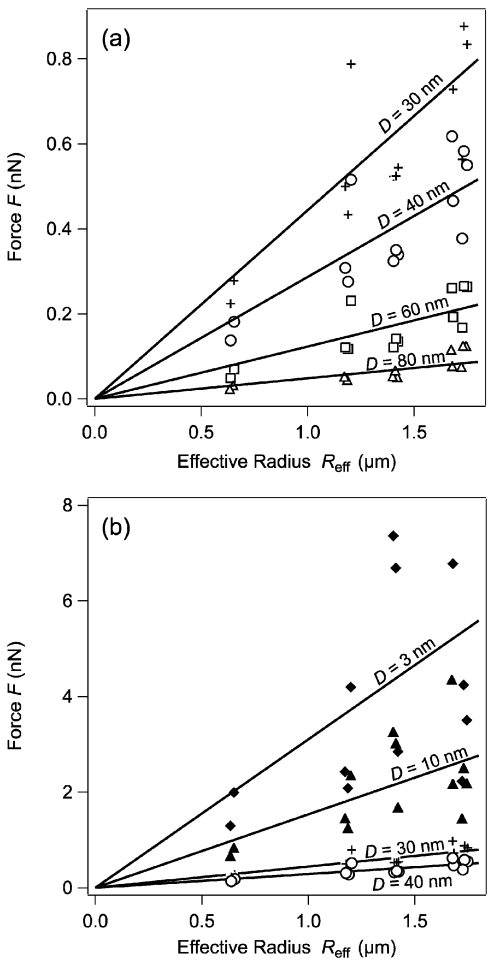

Fig. 4 Interaction forces F between silica particles as a function of the effective radius R_{eff} for separation distances D larger than 30 nm (a) and separation distances D smaller than 40 nm (b). The forces are measured in 0.1 mM KCl adjusted to pH 9.5. Solid lines are linear fits to the data with zero intercept.

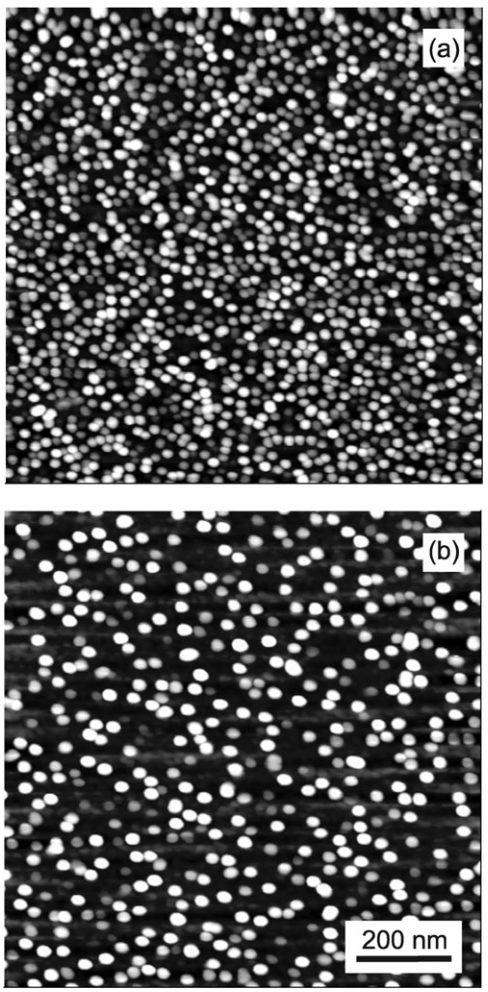

Fig. 5 AFM images adsorbed PAMAM G10 dendrimers on silicon wafers. Adsorbed at pH 4 from a KCl solution with a concentration of (a) 50 mM and (b) 5 mM. The dendrimers appear smaller in (a) due to the use of a selected sharp tip. The tip-convolution is more important in (b).

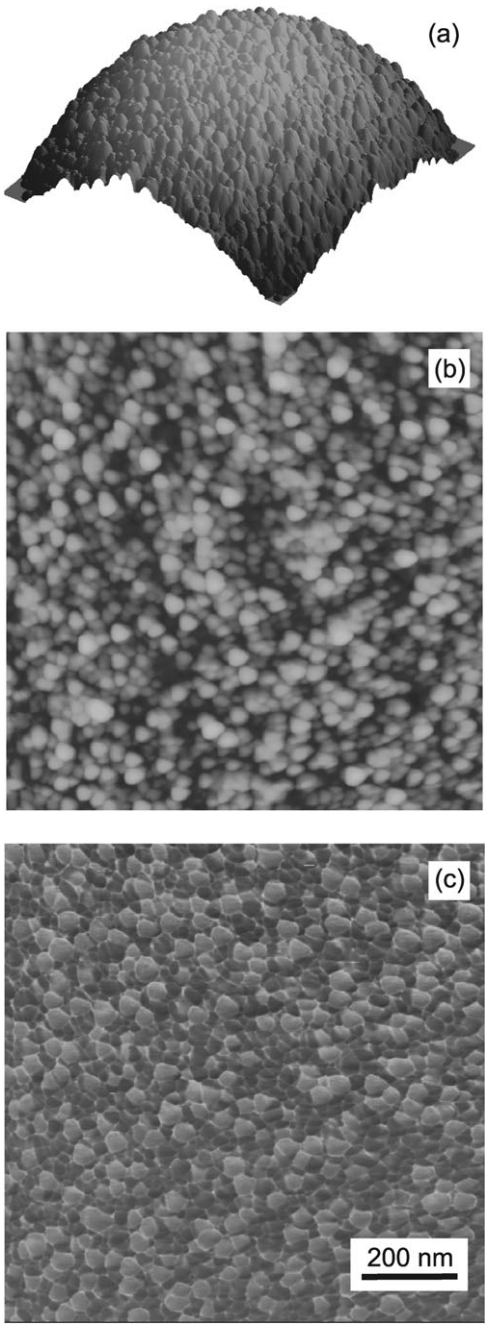

Fig. 6 AFM images of 6.8 μm silica particle with adsorbed PAMAM G10 dendrimers. The dendrimers were adsorbed from a 5 mM KCl solution at pH 4. Topographic image in (a) stereographic projection and (b) when flattened with a third order polynomial. (c) Phase image with a phase lag scale from 0 to 50°, whereby the bright parts represent the areas with a high phase lag.

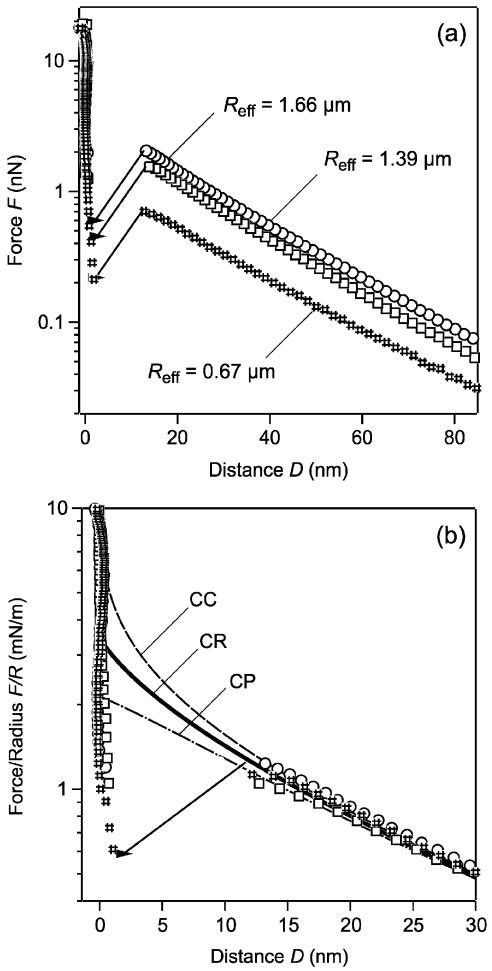

Fig. 7 Forces between pairs of silica particles with adsorbed G6 PAMAM dendrimers as a function of the separation distance D across a 0.1 mM aqueous KCl solution adjusted to pH 4.0. (a) Forces F for three different effective radii R_{eff}. (b) The same force curves normalized to the effective radius F/R_{eff}. Lines are best fits with the PB model with constant charge (CC), constant potential (CP), and constant regulation (CR) with $p = 0.5$. The fitted parameters are summarized in Table 2. The arrows indicate the jump-in.

G3, G6, and G10 to the negatively charged silica particles. Their structure is illustrated by AFM images of adsorbed G10 dendrimers on naturally oxidized silicon wafers shown in Fig. 5. The adsorbed dendrimers are arranged in a monolayer of low surface coverage, and they further show a liquid-like lateral order with a characteristic inter-dendrimer spacing.[30] This spacing decreases with decreasing dendrimer generation and increasing ionic strength, from which the adsorption was carried out. Fig. 5 illustrates the difference in the adsorbed amount and inter-dendrimer spacing when absorbing at pH 4 from 50 and 5 mM KCl. The adsorption at 50 mM yields a number concentration of 1.4×10^{15} m^{-2} and an inter-dendrimer spacing of 23 nm. These conditions correspond to the conditions used for the force measurements. Adsorption at 5 mM yields a number concentration of 5.2×10^{14} m^{-2} and an inter-dendrimer spacing of 49 nm. Adsorbed dendrimers on silica of generation G6 and lower cannot be resolved due to the roughness of the substrate.

The adsorption conditions in 5 mM KCl are necessary to obtain reliable AFM images of the dendrimers on the colloidal particles. The difficulties arise from the substantial roughness of these particles. Nevertheless, we have succeeded to image G10 dendrimers adsorbed onto 6.8 μm silica particle, as shown in Fig. 6. While the dendrimers cannot be easily detected in the

topographic images, their presence is most clearly revealed in the phase image (Fig. 6c). The phase image is sensitive to the viscoelastic properties of the sample, which permits to distinguish the soft dendrimers from the hard substrate. The number density of adsorbed dendrimers is 3.2×10^{14} m^{-2} on the particle compares relatively well with the value of 5.2×10^{14} m^{-2} on the flat silicon substrate, which was prepared under the same conditions as those discussed above. Phase images of the bare silica particle obtained under same conditions yields no contrast (Fig. 2c).

Force measurements between different spherical silica particles with adsorbed PAMAM dendrimer layers were performed in 0.1 mM KCl solution adjusted to pH 4. The resulting ionic strength is 0.2 mM. The irreversibly bound dendrimer layers were prepared by adsorption from dendrimer solutions of 10 mg L^{-1} in 50 mM KCl at pH 4. Fig. 7a shows typical force profiles for different pairs of silica particles precoated by G6 PAMAM dendrimers. The force profiles are not reversible upon approach and retraction. Upon approach, one observes repulsive interactions at large separation distances, a jump-in at smaller distances, and a repulsive force close to contact. The overlap of the diffuse layers is responsible for the repulsive forces at larger separation distances. The jump-in probably originates from patch-charge attractions, whereby the positively charged dendrimers are attracted by the negatively charged silica surface. Such attractive forces were proposed on theoretical grounds, and their range is comparable to the characteristic size of the surface heterogeneities.[7,45] The observed jump-in distances of about 10 nm are comparable to the expected inter-dendrimer spacing. However, the expected increase of the jump-in distance with the dendrimer generation could not be observed. The repulsive forces observed at short distances of a few nanometers are related to the compression and overlap of the adsorbed dendrimers. The retraction is characterized by a jump-out due to adhesion and isolated erratic single molecule events, typically at distances of 5–20 nm. Only the long-range repulsive part of the force profile measured upon approach is analyzed here.

Fig. 7b shows measured interaction forces relative to the effective radius for the dendrimer-coated surfaces. The normalized force profiles F/R_{eff} are again compared to solutions of the Poisson–Boltzmann equation with the boundary conditions of constant charge (CC), constant potential (CP), and constant regulation (CR). The solid lines are the best fits, whereby the measured decay lengths and diffuse layer potentials are summarized in Table 2. The decay lengths are in good agreement with the values predicted by the Debye–Hückel theory. The positive sign of the diffuse layer potential can be ascertained, since adsorbed PAMAM dendrimers lead to a charge reversal of negatively charged substrates.[46] The regulation parameters, which are in the range of 0.4–0.5, cannot be determined with confidence, since the jump-in masks the relevant part of the force profile.

The normalized force profiles F/R_{eff} shown in Fig. 7b collapse on a common curve, confirming the validity of the Derjaguin approximation. More detailed confirmation is given in Fig. 8. The interaction force is shown as a function of the effective radius at various separation distances for the three generations G3, G6, and G10. For all three dendrimer generations, the force is found to be proportional to the effective radius. Again, the validity of the Derjaguin approximation is confirmed.

Given the charge heterogeneity of the substrates, the validity of this approximation is somewhat surprising. Its breakdown might be suspected, since the characteristic size of the surface heterogeneities is on the order of 10 nm, and the forces are being probed down to distances of 30 nm. In spite of the fact that these two length scales become comparable, the Derjaguin approximation remains valid.

4. Conclusions

The Derjaguin approximation was confirmed by measuring interaction forces between colloidal particles of different size but of identical composition across an aqueous solution with an AFM. This approximation holds even at small distances,

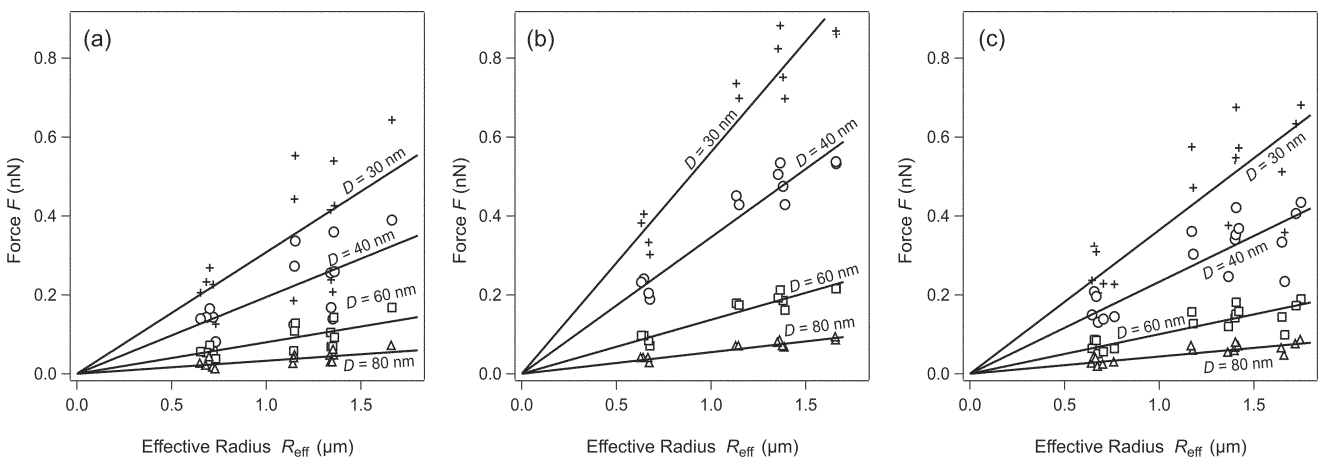

Fig. 8 Interaction forces F between silica particles with adsorbed layers of PAMAM dendrimers measured as a function of the effective radius R_{eff} for a given separation distance. The forces are measured in 0.1 mM KCl adjusted to pH 4.0. Solid lines are linear fits to the data with zero intercept. Generations (a) G3, (b) G6, and (c) G10.

which are comparable to the surface roughness or the characteristic distance of a heterogeneously charged substrate. Derjaguin approximation is thus surprisingly robust, even for rather heterogeneous substrates.

Under appropriate conditions, the Derjaguin approximation will necessarily break down. Its failure is expected for interactions between AFM tips and flat substrates, where the tip radius is comparable to the range of the interaction.[27] The situation is less clear for heterogeneous substrates. Based on theoretical arguments, this approximation was suggested to be valid at small distances.[7] The present study clearly corroborates this point, as the Derjaguin approximation remains valid for heterogeneous substrates down to distances comparable to the lateral length scale of the surface heterogeneities. On the other hand, for some substrates with highly pronounced lateral heterogeneities, some deviations could be observed. However, such cases are hard to find and seem to be quite exceptional, and for this reason could not be analyzed in detail so far.

Acknowledgements

This research was supported by the Swiss National Science Foundation and the University of Geneva.

References

1 W. B. Russel, D. A. Saville and W. R. Schowalter, *Colloidal Dispersions*, Cambridge University Press, Cambridge, 1989.
2 J. Israelachvili, *Intermolecular and Surface Forces*, Academic Press, London, 1992.
3 C. Bonnet-Gonnet, L. Belloni and B. Cabane, *Langmuir*, 1994, **10**, 4012–4021.
4 T. Palberg, W. Monch, F. Bitzer, R. Piazza and T. Bellini, *Phys. Rev. Lett.*, 1995, **74**, 4555–4558.
5 S. H. Behrens, D. I. Christl, R. Emmerzael, P. Schurtenberger and M. Borkovec, *Langmuir*, 2000, **16**, 2566–2575.
6 S. L. Carnie, D. Y. C. Chan and J. S. Gunning, *Langmuir*, 1994, **10**, 2993–3009.
7 J. Stankovich and S. L. Carnie, *J. Colloid Interface Sci.*, 1999, **216**, 329–347.
8 L. Suresh and J. Y. Walz, *J. Colloid Interface Sci.*, 1996, **183**, 199–213.
9 B. Gotzelmann, R. Evans and S. Dietrich, *Phys. Rev. E*, 1998, **57**, 6785–6800.
10 S. Biggs, D. C. Prieve and R. R. Dagastine, *Langmuir*, 2005, **21**, 5421–5428.
11 B. V. Derjaguin, *Kolloid Z.*, 1934, **69**, 155–164.
12 J. E. Sader, S. L. Carnie and D. Y. C. Chan, *J. Colloid Interface Sci.*, 1995, **171**, 46–54.
13 S. Bhattacharjee and M. Elimelech, *J. Colloid Interface Sci.*, 1997, **193**, 273–285.
14 R. M. Pashley, *J. Colloid Interface Sci.*, 1981, **83**, 531–546.
15 P. M. Claesson, T. Ederth, V. Bergeron and M. W. Rutland, *Adv. Colloid Interface Sci.*, 1996, **67**, 119–183.
16 W. A. Ducker, T. J. Senden and R. M. Pashley, *Nature*, 1991, **353**, 239–241.
17 H. J. Butt, *Biophys. J.*, 1991, **60**, 1438–1444.
18 H. J. Butt, In *Encyclopedia of Electrochemistry*, ed. A. J. Bardand and M. Stratmann, Wiley-VCH, Weinheim, 2003, vol. 1, pp. 225–252.
19 B. Cappella and G. Dietler, *Surf. Sci. Rep.*, 1999, **34**, 1–104.
20 I. L. Radtchenko, G. Papastavrou and M. Borkovec, *Biomacromolecules*, 2005, **6**, 3057–3066.
21 M. Giesbers, J. M. Kleijn and M. A. Cohen Stuart, *J. Colloid Interface Sci.*, 2002, **252**, 138–148.
22 I. Larson, C. J. Drummond, D. Y. C. Chan and F. Grieser, *J. Phys. Chem.*, 1995, **99**, 2114–2118.
23 G. Toikka, R. A. Hayes and J. Ralston, *Langmuir*, 1996, **12**, 3783–3788.
24 G. Toikka, R. A. Hayes and J. Ralston, *Colloids Surf., A*, 1998, **141**, 3–8.
25 R. F. Considine and C. J. Drummond, *Langmuir*, 2001, **17**, 7777–7783.
26 R. F. Considine, D. R. Dixon and C. J. Drummond, *Langmuir*, 2000, **16**, 1323–1330.
27 B. A. Todd and S. J. Eppell, *Langmuir*, 2004, **20**, 4892–4897.
28 W. Kern and D. A. Puotinen, *RCA Rev.*, 1970, **31**, 187.
29 D. Cakara, J. Kleimann and M. Borkovec, *Macromolecules*, 2003, **36**, 4201–4207.
30 R. Pericet-Camara, G. Papastavrou and M. Borkovec, *Langmuir*, 2004, **20**, 3264–3270.
31 V. V. Tsukruk, F. Rinderspacher and V. N. Bliznyuk, *Langmuir*, 1997, **13**, 2171–2176.
32 J. P. Cleveland, S. Manne, D. Bocek and P. K. Hansma, *Rev. Sci. Instrum.*, 1993, **64**, 403–405.
33 J. L. Hutter and J. Bechhoefer, *Rev. Sci. Instrum.*, 1993, **64**, 1868–1873.
34 J. E. Sader, J. W. M. Chon and P. Mulvaney, *Rev. Sci. Instrum.*, 1999, **70**, 3967–3969.
35 R. Proksch, T. E. Schaffer, J. P. Cleveland, R. C. Callahan and M. B. Viani, *Nanotechnology*, 2004, **15**, 1344–1350.
36 J. J. Adler, Y. I. Rabinovich and B. M. Moudgil, *J. Colloid Interface Sci.*, 2001, **237**, 249–258.
37 G. Vigil, Z. H. Xu, S. Steinberg and J. Israelachvili, *J. Colloid Interface Sci.*, 1994, **165**, 367–385.
38 R. Pericet-Camara, G. Papastavrou, S. H. Behrens and M. Borkovec, *J. Phys. Chem. B*, 2004, **108**, 19467–19475.
39 M. Kobayashi, F. Juillerat, P. Galletto, P. Bowen and M. Borkovec, *Langmuir*, 2005, **21**, 5761–5769.
40 P. G. Hartley, I. Larson and P. J. Scales, *Langmuir*, 1997, **13**, 2207–2214.
41 P. J. Scales, F. Grieser, T. W. Healy, L. R. White and D. Y. C. Chan, *Langmuir*, 1992, **8**, 965–974.
42 G. Toikka and R. A. Hayes, *J. Colloid Interface Sci.*, 1997, **191**, 102–109.
43 I. Larson, C. J. Drummond, D. Y. C. Chan and F. Grieser, *Langmuir*, 1997, **13**, 2109–2112.
44 S. H. Behrens and M. Borkovec, *J. Phys. Chem. B*, 1999, **103**, 2918–2928.
45 S. J. Miklavic, D. Y. C. Chan, L. R. White and T. W. Healy, *J. Phys. Chem.*, 1994, **98**, 9022–9032.
46 W. Lin, P. Galletto and M. Borkovec, *Langmuir*, 2004, **20**, 7465–7473.

